Quantum nonlinear four-wave mixing with a single atom in an optical cavity

Haytham Chibani*
Max-Planck-Institut für Quantenoptik, Hans-Kopfermann-Str. 1, D-85748 Garching, Germany
(Dated: May 14, 2017)

Single atom cavity quantum electrodynamics grants access to nonclassical photon statistics, while electromagnetically induced transparency exhibits a dark state of long coherence time. The combination of the two produces a new light field via four-wave mixing that shows long-lived quantum statistics. We observe the new field in the emission from the cavity as a beat with the probe light that together with the control beam and the cavity vacuum is driving the four-wave mixing process. Moreover, the control field allows us to tune the new light field from antibunching to bunching, demonstrating our all-optical control over the photon-pair emission.

Nonlinear optics requires media in which the dielectric polarization responds nonlinearly to the electric field of the light. In conventional media, this occurs for very high intensities. To bring nonlinear optics to the quantum domain of single photons, giant nonlinearities like those provided by atomic ensembles in Rydberg states [1–5] or single atoms in optical resonators [6–8] are mandatory. Indeed, such systems can produce quantum fields [9–11], in particular those containing single photons [12–14]. However, these achievements have so far exploited only a small subset of the arsenal provided by nonlinear optics. Incorporating higher-order effects like four-wave mixing to generate and control more complex quantum light fields would broaden the application potential of quantum nonlinear optics towards a fully coherent manipulation of both the intensity and the frequency of quantum light fields.

Here we report on a cavity quantum electrodynamics (QED) experiment where a single atom strongly coupled to a high-finesse optical resonator emits a new quantum field by four-wave mixing. Phase matching is not required as the atom constitutes a medium with vanishing length. The new field is resonantly emitted into the cavity vacuum, and is induced by shining probe and control beams onto the cavity and the atom, respectively. The control field guarantees electromagnetically induced transparency (EIT) for cavity light [15–17]. The probe field addresses a normal mode of the system and thus experiences photon blockade [9], a genuine quantum-mechanical effect. The coherent interplay between all light fields produces a long-lived atomic superposition state that leads to an equally long-lived non-classical feature in the light emitted from the cavity. The quantum character of this effect can be optically controlled with the control beam. Our system with its unique combination of cavity QED and cavity EIT could be a novel building block of a network of atom-cavity systems with the aim of controlling the predicted phase transition of light into an ordered Mott-insulator-like state of photons [18–20].

The principle of our experiment works as follows. We consider a single Λ-type three-level atom with equal polarization decay rate $\gamma/2$ from the excited state $|e\rangle$ to the two ground states $|g_1\rangle$ and $|g_2\rangle$. The atom is held inside a cavity with a field decay rate κ and is exposed to a control laser field coming from the side as depicted in Fig. 1 (a). The cavity is strongly coupled to the atomic transition $|g_1\rangle \rightarrow |e\rangle$ with a coupling strength $g_0 > (\kappa, \gamma)$. A control laser field at frequency ω_{con} drives the $|g_2\rangle \rightarrow |e\rangle$ transition resonantly with a Rabi frequency Ω_{con}. Together, the vacuum field of the cavity and the control laser establish a cavity EIT configuration.

Figure 1(b) shows the new eigenstates of the system, consisting of a ladder of triplets with ladder steps n representing the number of excitations in the system. A detailed theoretical treatment of the considered system can be found in [21]. With the ground state $|\Psi_0^0\rangle = |g_1, 0\rangle$, all other eigenstates with $n \geq 1$ can be written as

$$|\Psi_n^{\pm}\rangle \propto |g_1, n\rangle \pm \frac{g_{n,\text{eff}}}{\sqrt{n} g_0} |e, n-1\rangle + \frac{\Omega_{con}}{\sqrt{n} g_0} |g_2, n-1\rangle \quad (1)$$

$$|\Psi_n^0\rangle \propto |g_1, n\rangle - \frac{\sqrt{n} g_0}{\Omega_{con}} |g_2, n-1\rangle, \quad (2)$$

where $g_{n,\text{eff}} = \sqrt{n g_0^2 + \Omega_{con}^2}$ is the effective atom-cavity coupling strength. The states $|\Psi_n^{\pm}\rangle$ represent superposition states in which one excitation is shared between the atom and the cavity, similar to the dressed states of a two-level atom strongly coupled to a cavity, but with an admixture of the second ground state $|g_2\rangle$. Note that the splitting of the $|\Psi_n^{\pm}\rangle$ states scales with twice the effective atom-cavity coupling $g_{n,\text{eff}}$. Therefore, the control field Rabi frequency Ω_{con} can be used as a control knob to tune $g_{n,\text{eff}}$ and consequently the spectral positions of the $|\Psi_n^{\pm}\rangle$ eigenstates. The third series of eigenstates $|\Psi_n^0\rangle$, completing the triplets, represent the cavity EIT state, in which the atom is in a "dark" superposition of the states $|g_1\rangle$ and $|g_2\rangle$ with no population in the excited state $|e\rangle$. For our parameters, these states are resonant with the empty cavity. Thus, a probe laser at frequency ω_{probe} driving the system with a driving strength η on resonance with the empty cavity will simply be transmitted. Driving the system close to resonance with the states $|\Psi_1^{\pm}\rangle$ will induce a coherent

four-wave mixing process, which we will now discuss in detail.

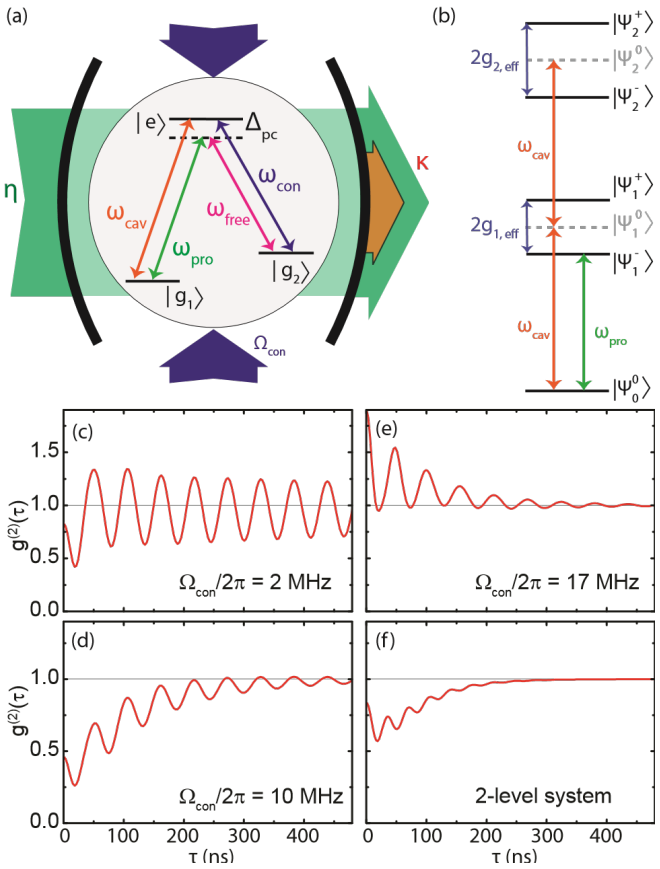

FIG. 1. (Color online). (a) A single Λ-type three-level atom with two ground states $|g_1\rangle$ and $|g_2\rangle$ and a an excited state $|e\rangle$ is positioned at the center of an optical cavity with a decay rate κ. A control beam, transverse to the cavity axis, drives the $|g_2\rangle \rightarrow |e\rangle$ transition resonantly with a Rabi frequency Ω_{con} which together with the cavity vacuum (ω_{cav}) establish the cavity EIT condition. A probe laser at frequency ω_{probe} and with a driving strength η is driving the four-wave mixing process, in which two new fields at frequencies ω_{free} and ω_{cav} are emitted. (b) Energy levels of the strongly coupled cavity EIT system shown up to the second manifold. $|\Psi_n^0\rangle$ are dark states of the cavity EIT system and $|\Psi_n^{\pm}\rangle$ the cavity QED like dressed eigenstates. (c)-(e) Numerical simulations of the time-dependent second-order correlation function $g^{(2)}(\tau)$ for different control field Rabi frequencies Ω_{con} showing the beating of the probe field with the new field emitted into the cavity. Depending on Ω_{con} the photon pair correlation shows antibunching or bunching. The coherence time of the beat exceeds the coherence time expected for a two-level atom strongly coupled to the cavity shown for comparison in (f).

In the four-wave mixing process the atom absorbs light from the probe and control beams and emits a field at frequency ω_{cav} into the cavity mode as well as one at frequency ω_{free} into free space, compare Fig. 1(a). The role of the cavity vacuum in this process is twofold. Firstly, it ensures the EIT condition by coupling the states $|g_1\rangle$ and $|e\rangle$, and therefore driving, together with the control and probe beams, the coherent emission of the light field at frequency ω_{free}. Secondly, it stimulates the light field at frequency ω_{cav} that is emitted in the four-wave mixing process into the cavity vacuum. This new field is closely related to the vacuum induced transparency field [22]. Energy conservation yields the following condition for the new fields $\omega_{cav} - \omega_{con} = \omega_{probe} - \omega_{free} = \Delta_{g_{12}}$, where $\Delta_{g_{12}}$ is the energy difference between the two ground states. While it is hard to detect the generated field, with a frequency ω_{free}, that is emitted into modes outside the cavity, the emission into the cavity mode facilitates the detection of the other generated field with a frequency ω_{cav}. It is superposed with the probe light, leading to a beating of the two light fields that can be detected outside the cavity.

The generation of four-wave mixing can be demonstrated by extracting the beat frequency from intensity correlation measurements $g^{(2)}(\tau) = \langle n(\tau)n\rangle/\langle n\rangle^2$ where n is the photon number operator, which allow at the same time to reveal the quantum character of the field. To illustrate this, we show in Fig. 1(c)-(e) numerical simulations of $g^{(2)}(\tau)$ for parameters corresponding to our ideal experimental values $\{g_0, \lambda, \kappa\}/2\pi = \{14, 3, 2\}$ MHz, with a probe laser driving strength $\eta \approx \kappa$ and a probe-cavity detuning $\Delta_{pc}/2\pi = (\omega_{probe} - \omega_{cav})/2\pi = -18$ MHz for different control field Rabi frequencies Ω_{con}. For all values of Ω_{con}, a strong oscillation is visible that comes from the superposition of the probe field with the new field which shows a beat frequency that matches the condition $\omega_{beat} = |\omega_{con} + \Delta_{g_{12}} - \omega_{probe}| = \Delta_{pc}$. Remarkably, the coherence time of this oscillation is much longer than any inverse decay rate of the system. For comparison, we show in Fig. 1(f) the two-level atom cavity QED case with the same parameters, but at $\Delta_{pc} = -g_0$, at resonance with the lower normal mode. In this case the probe field experiences photon blockade, resulting in photon antibunching. Moreover, in Fig. 1(f) an oscillation is visible, that has a frequency corresponding to the normal mode splitting $2g_0$ [8], and the steady state of uncorrelated photons is reached on a time scale that is entirely determined by the linewidth of the normal modes $(\kappa+\gamma)/2$. In contrast, for all drawn cavity EIT cases, Fig. 1(c)-(e), the beat of the probe field with the new intracavity field is observable for longer timescales, which points towards the long coherence time of the cavity EIT dark state on which the four-wave mixing process is based on [23, 24]. However, for growing Ω_{con}, the coherence time of the beat decreases, since the linewidth of the EIT dark state, given by $\Gamma_{|\Psi_1^0\rangle} = \frac{\kappa\Omega_c^2}{\Omega_c^2+g_0^2}$, is growing at the same time up to the limit set by κ.

More complex is the dependence of the value of the equal-time photon-pair correlation $g^{(2)}(0)$ on the control Rabi frequency Ω_{con}. By changing the effective atom-cavity coupling $g_{n,\text{eff}}$, it is changing the spectral position

of the eigenstates. Therefore, the probe laser, that is without control light red detuned from the lowest dressed state, as in Fig.1(c), will be shifted into resonance with the first manifold for intermediate values of Ω_{con} like shown in Fig.1(d), experiencing photon blockade, since it is detuned from higher lying eigenstates [9]. Increasing the control field Rabi frequency Ω_{con} further will shift the eigenstates such that the probe will be on resonance with the second manifold, as shown in Fig.1(e). Now, two photons can be absorbed at once, and the probe beam will experience photon bunching [25]. As already pointed out in [21], the simulations show that by tuning the control field Rabi frequency one can achieve a good control over the probability of transmitting photon pairs, which is equivalent with controlling the photon statistics of an initially coherent probe beam.

To observe the predicted effects in the experiment, we load optically cooled [26] single ^{87}Rb atoms ($\gamma/2\pi = 3\,$MHz) into a high-finesse ($\mathcal{F} = 195,000$) Fabry-Perot cavity of length 200 μm yielding a cavity field decay rate $\kappa/2\pi = 2\,$MHz. Strong coupling is achieved by choosing as $|g_1\rangle$ the state $5S_{1/2}, F = 1$ and as $|e\rangle$ the state $5P_{3/2}, F' = 2$ transition of the D2 line in ^{87}Rb, for which the maximum rate of atom-cavity coupling is $g_0/2\pi = 14.3$ MHz for the $(F = 1, m_F = 1) \rightarrow (F' = 2, m_F = 2)$ transition. As state $|g_2\rangle$ we chose the state $5S_{1/2}, F = 2$. The control field drives the atom transversely to the cavity axis, retroreflected and in a lin $\perp$ lin configuration. The atom is held in a pair of crossed red-detuned standing-wave dipole traps, one linearly polarized at 784 nm perpendicular to the cavity, and one circularly polarized intra-cavity trap at 786 nm. The intra-cavity trap is also used to stabilize the cavity to the $|g_1\rangle$ to $|e\rangle$ transition with a detuning of about 16 MHz with respect to the bare atomic states, such that the a.c. Stark shift induced by the dipole traps is approximately compensated, resulting in an atom-cavity detuning of only about 1 MHz, depending on the respective Zeeman substate. The coupled system is driven by a circularly polarized probe laser with a driving strength $\eta \approx \kappa$, putting the system in the low driving limit.

Upon detection of the atom we start with a sequence of alternating cool (20ms) [26] and probe intervals (200 μs) that we repeat as long as the atom stays trapped. During the probe intervals only the control and probe beams are applied. To make sure that the atom is sufficiently well coupled to the cavity, we check the coupling before and after the probe interval [27] for about 200 μs, and include only probe intervals in the evaluation of the data that passed this test.

We first start by demonstrating strong coupling of cavity QED for a single atom by measuring transmission through the cavity as a function of the probe field frequency, with no presence of the control field and with the atom prepared in the $|g_1\rangle$ ground state. Note that we are probing an open transition here, meaning that

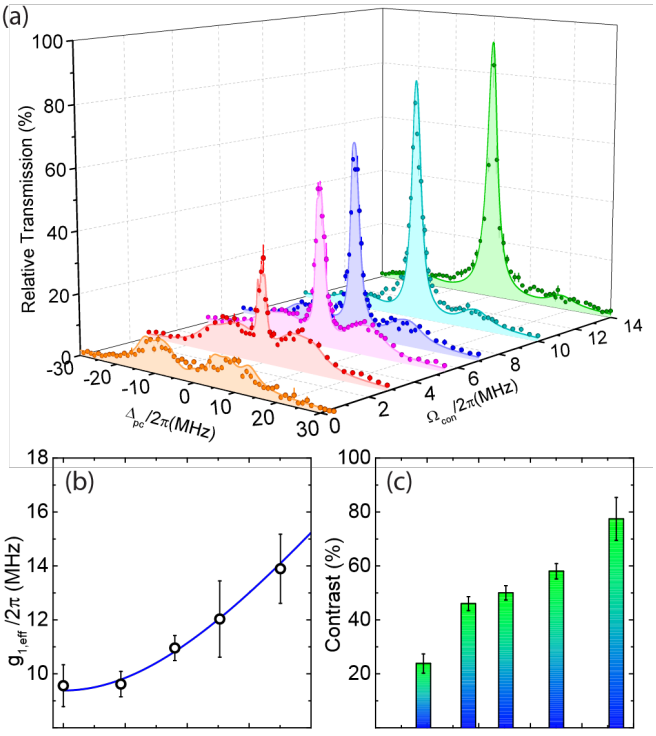

FIG. 2. (Color online.) (a) Probe transmission spectra for different control field Rabi frequencies. Dots represent the data while solid lines are theoretical predictions for the respective control field Rabi frequency. (b) The effective atom-cavity coupling $g_{1,\mathrm{eff}}$ is enhanced as the control Rabi frequency Ω_{con} is increased. (c) The on-off contrast of the single-atom transparency window at the empty cavity resonance increases with the control field Rabi frequency to about 80 %.

state $|e\rangle$ can decay into state $|g_2\rangle$i which is not coupled to the cavity. Therefore, a repumper ($F = 2 \rightarrow F' = 1$) is applied simultaneously to the probe to keep the atom in the cavity-coupled state $|g_1\rangle$. Then the atom can be considered as an effective two-level system coupled to the cavity with new energy eigenstates given by the Jaynes-Cummings model. In the spectrum we observe a vacuum-Rabi splitting of about $2g/2\pi \approx 19$ MHz along with a significant drop in the transmission at the empty cavity resonance ($\Delta_{pc} = 0$) which is a hallmark of strong coupling (Fig.2(a), dots for $\Omega_{con} = 0$). We do not reach the maximal coupling rate g_0, since we do not prepare the system in the Zeeman substate $F = 1, m_F = 1$. Instead, the atom is distributed over all m_F substates which all have different maximal coupling rates to the cavity, $g_{0,mF=-1,0,1}/2\pi = \{5.8, 9.2, 14.3\}$ MHz, resulting in a mean coupling rate that is lower than g_0. The solid line with the filled area is a fitted theory, that includes three different Λ-schemes from all possible initial m_F substates weighted differently with respect to their expected populations as well as a small residual transmission at the empty cavity frequency which could result from the non zero probability of the atom being in a dark state.

Next, we turn on the control field to put the system in EIT configuration. Figure 2(a) shows cavity transmission spectra obtained for different control field Rabi frequencies, dots are data points, solid lines with filled area are theory predictions. We observe the presence of a cavity EIT window at the empty cavity resonance which grows in amplitude to almost full transmission as the control field Rabi frequency is increased. The control field on-off contrast at the empty-cavity resonance grows with the control field power to about 80 % (compare with Fig.2(c)), which is unprecedented for a single emitter EIT medium [15, 16, 28]. Moreover, the normal mode splitting $2g_{1,\text{eff}}$ also increases as the control field Rabi frequency is increased. We find that the spectral position of the normal modes, that we extract from the fitted theory, follows a square root behavior with Ω_{con}^2 as predicted, see Fig.2 (b). We then use this dependency to calibrate the applied control field power to the control field Rabi frequencies seen by the atom. With the cavity EIT spectra we demonstrate our ability to optically control the transmission of probe photons through the atom-cavity system, which is an average observable, and at the same time to spectrally tune the system's resonances by simply varying the control field power.

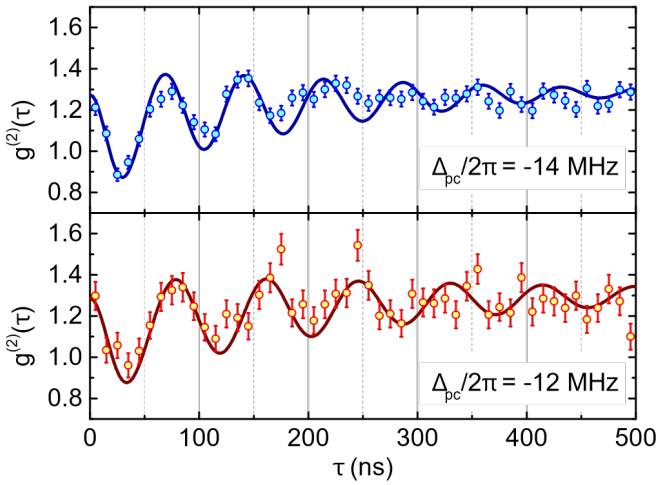

FIG. 3. (Color online). Measured two-photon correlations $g^{(2)}(\tau)$ compared to theoretical expectations in (a) at $\Delta_{pc}/2\pi = -14$ MHz and $\Omega_{con}/2\pi = 4$ MHz, and in (b) at $\Delta_{pc}/2\pi = -12$ MHz and $\Omega_{con}/2\pi = 4.3$ MHz. Dots are representing experimental data with statistical error bars, solid lines are showing theory.

With the prerequisite of cavity EIT in the strong coupling regime at hand, we now report measurements of the intensity correlation function of the transmitted probe light. In Figure 3, we show the renormalized two-photon correlation function $\widetilde{g}^{(2)}(\tau) = g^{(2)}(\tau)/g^{(2)}_{norm}$ (dots represent experimental data, solid lines theory) for two different probe-cavity detunings $\Delta_{pc}/2\pi = -14$ MHz and -12 MHz, and for similar control field Rabi frequencies $\Omega_{con}/2\pi$ of 4.0 MHz and 4.3 MHz, respectively. In both cases $\widetilde{g}^{(2)}(\tau)$ is dominated by an oscillation at the probe-cavity detuning Δ_{pc}, the beat frequency of the new field and the probe light. Renormalization is necessary since $g^{(2)}(\tau)$ is settling at a value above one, due to the motion of the atom in the trap and variations of the atomic position in the cavity mode from one experimental realization to the next [9]. We therefore renormalize $g^{(2)}(\tau)$ to the average level of classically correlated photons $g^{(2)}_{norm} = \frac{1}{\tau_2-\tau_1} \cdot \int_{\tau_1}^{\tau_2} g^{(2)}(\tau)d\tau$, for times between $\tau_1 = 400$ ns and $\tau_2 = 600$ ns, for which the reduction of correlation events due to the atomic oscillation in the trap is still small, but the beat between the probe and new field has mostly decayed. The solid lines show expectations from our theoretical model that includes three lambda systems. However, we notice that the observed oscillations have a longer coherence time than the dissipation rates of the system κ and γ suggesting their EIT origin. In fact, by performing a Fourier transformation of the date, we find for both measurements indeed Δ_{pc} as central frequency with a width of $\delta \approx 0.8$ MHz corresponding to the decay time of 200 ns of the observed oscillations. This is more than a factor of 3 larger than the coherence time obtained with a usual two-level cavity QED system with similar parameters, where the relaxation time of the correlation function would be $2/(\kappa+\gamma) = 63$ ns.

Both photon-photon correlations shown above, already show the quantum nature of the field emitted from the cavity, since they violate the inequalities allowed for classical correlations: $|\widetilde{g}^{(2)}(\tau) - 1| \leq |\widetilde{g}^{(2)}(0) - 1|$ [29, 30]. However, we want to demonstrate that we are able to also influence the probability of photon pair emissions, which is proportional to the equal-time photon-photon correlation $\widetilde{g}^{(2)}(0)$. We have carried out measurements for different control Rabi frequencies but for the same probe frequency, which are summarized in Fig. 4. The non-classical behavior of the transmitted field is clearly visible for $\Omega_{con}/2\pi = 4.3$ MHz, with $\widetilde{g}^{(2)}(0) = 0.82 \pm 0.05$ which is a signature of photon blockade and photon anti-bunching as can be seen in the upper inset of Fig. 4. This is a result of the probe laser frequency (at $\Delta_{pc}/2\pi = -14$ MHz) being near-resonant to the lower normal-mode frequency thereby increasing the steady-state population in the eigenstate $|\Psi_1^-\rangle$ and thus the single photon emission probability. Increasing the control field Rabi frequency to $\Omega_{con}/2\pi = 12.3$ MHz transforms the photon blockade into a two-photon gateway [25] with $\widetilde{g}^{(2)}(0) = 1.3 \pm 0.1$ with a higher probability of photon pair emission for the same input field frequency. In fact, this is due to a $g_{1,\text{eff}}/2\pi \approx 15.5$ MHz which would bring the probe laser frequency closer to resonance with the second manifold of the cavity EIT ladder and therefore increase the steady-state population in the $|\Psi_2^-\rangle$ explaining the behavior observed in the lower inset of Fig. 4.

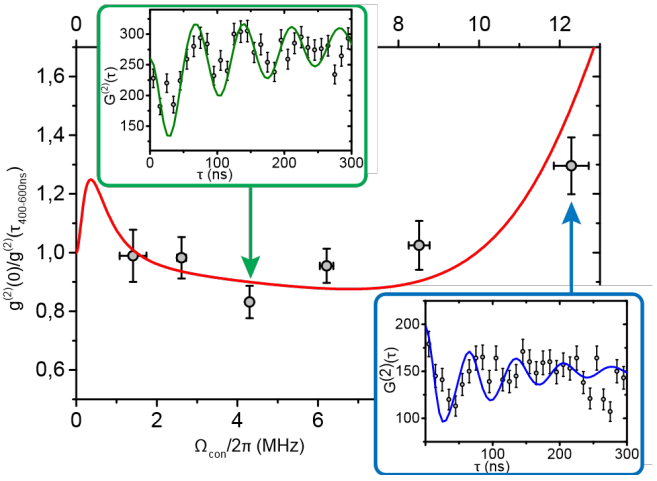

FIG. 4. (Color online). Optical control of photon pair emission for $\Delta_{pc}/2\pi = -14$ MHz. By changing Ω_{con}, we can change the photon statistics of the light transmitted through the cavity. For $\Omega_{con}/2\pi = 4.3$ MHz, we measure antibunching (compare upper inset), while for $\Omega_{con}/2\pi = 12$ MHz we observe photon bunching (compare lower inset). The solid red line shows the theoretical predictions for our parameters and the inset figures show the corresponding unnormalized second-order correlations $G^{(2)}(\tau)$.

In conclusion, we demonstrated that by combining single-atom cavity QED in the strong coupling regime with single-atom cavity EIT we could generate multiple non-classical photon statistics of the transmitted field which are optically controllable. In addition, the generated new field at the empty cavity resonance frequency confirms the potential of the considered system to achieve high optical nonlinearities. In future experiments, we plan to bring this optical control of photon statistics to the single photon level [31, 32].

* Electronic address: haytham.chibani@gmail.com

[1] S. Sevinçli, N. Henkel, C. Ates, and T. Pohl, Phys. Rev. Lett. **107**, 153001 (2011).

[2] D. E. Chang, V. Gritsev, G. Morigi, V. Vuletić, M. D. Lukin, and E. A. Demler, Nature Physics **4**, 884–889 (2008).

[3] A. V. Gorshkov, J. Otterbach, M. Fleischhauer, T. Pohl, and M. D. Lukin, Phys. Rev. Lett. **107**, 133602 (2011).

[4] S. Baur, D. Tiarks, G. Rempe, and S. Dürr, Phys. Rev. Lett. **112**, 073901 (2014).

[5] J. Otterbach, M. Moos, D. Muth, and M. Fleischhauer, Phys. Rev. Lett. **111**, 113001 (2013).

[6] C. Sames, H. Chibani, C. Hamsen, P. A. Altin, T. Wilk, and G. Rempe; Phys. Rev. Lett. 112, 043601 (2014).

[7] A. Rauschenbeutel, G. Nogues, S. Osnaghi, P. Bertet, M. Brune, J. M. Raimond, and S. Haroche, Phys. Rev. Lett. 83, 5166 (1999).

[8] M. Koch, C. Sames, M. Balbach, H. Chibani, A. Kubanek, K. Murr, T. Wilk, and G. Rempe, Phys. Rev. Lett. **107**, 023601 (2011).

[9] K.M. Birnbaum, A. Boca, R. Miller, A.D. Boozer, T. E. Northup, and H. J. Kimble, Nature **436**, 87-90 (2005).

[10] A. Ourjoumstev, A. Kubanek, M. Koch, C. Sames, P. W. H. Pinkse, G. Rempe, and K. Murr, Nature 474, 623-626 (2011).

[11] S. L. Mielke, G. T. Foster, and L. A. Orozco, Phys. Rev. Lett. **80**, 3948 (1998).

[12] A. Kuhn, M. Hennrich, and G. Rempe, Phys. Rev. Lett. **89**, 067901 (2002).

[13] J. McKeever, A. Boca, A. D. Boozer, R. Miller, J. R. Buck, A. Kuzmich, and H. J. Kimble, Science **303**, 1992 (2004).

[14] M. Hijlkema, B. Weber, H. P. Specht, S. C. Webster, A. Kuhn, and G. Rempe, Nature Phys. **3**, 253 (2007).

[15] M. Mücke, E. Figueroa, J. Bochmann, C. Hahn, K. Murr, S. Ritter, C. J. Villas-Boas, and G. Rempe, Nature **465**, 755-758 (2010).

[16] T. Kampschulte, W. Alt, S. Brakhane, M. Eckstein, R. Reimann, A. Widera, and D. Meschede, Phys. Rev. Lett. **105**, 153603 (2010).

[17] M. Albert, A. Dantan, and M. Drewsen, Nature Photonics **5**, 633-636 (2011).

[18] M. J. Hartmann, F. G. S. L. Brandao, and M. B. Plenio, Nature Physics **2**, 849 (2006).

[19] A. D. Greentree, C. Tahan, J. H. Cole, and L. C. L. Hollenberg, Nature Physics **2**, 856 (2006).

[20] D. G. Angelakis, M. F. Santos, and S. Bose, Phys. Rev. A. **76**, 031805 (2007).

[21] J.A. Souza, E. Figueroa, H. Chibani, C.J. Villas-Boas, and G. Rempe, Phys. Rev. Lett. **111**, 113602 (2013).

[22] H. Tanji-Suzuki, W. Chen, R. Landig, J. Simon, and V. Vuletić Science **333**, 1266-1269 (2011).

[23] M. D. Lukin, M. Fleischhauer, A. S. Zibrov, H. G. Robinson, V. L. Velichansky, L. Hollberg, and M. O. Scully, Phys. Rev. Lett. **79**, 2959 (1997).

[24] Y. Li, and M. Xiao, Opt. Lett. **21**, 1064-1066 (1996).

[25] A. Kubanek, A. Ourjoumtsev, I. Schuster, M. Koch, P. W. H. Pinkse, K. Murr, and G. Rempe, Phys. Rev. Lett. **101**, 203602 (2008).

[26] S. Nußmann, K. Murr, M. Hijlkema, B. Weber, A. Kuhn, and G. Rempe, Nature Physics **1**, 122-126 (2005).

[27] P. Maunz, T. Puppe, I. Schuster, N. Syassen, P. W. H. Pinkse, and G. Rempe, Phys. Rev. Lett. **94**, 033002 (2005).

[28] L. Slodička, G. Hétet, S. Gerber, M. Hennrich, and R. Blatt, Phys. Rev. Lett. **105**, 153604 (2010).

[29] R. J. Brecha, P. R. Rice, and M. Xiao, Phys. Rev. A **59**, 2392-2417 (1999).

[30] H. J. Carmichael, R. J. Brecha, and P. R. Rice, Opt. Commun. **82**, 73-79 (1991).

[31] A. Imamoğlu, H. Schmidt, G. Woods, and M. Deutsch, Phys. Rev. Lett. **79**, 1467 (1997).

[32] P. Grangier, D. F. Walls, and K. M. Gheri, Phys. Rev. Lett. **81**, 2833 (1998).